

# Light elements in the Martian core

Yinfang Yang<sup>1,2</sup> · Shuangmeng Zhai<sup>1</sup> 

Received: 2 June 2025 / Revised: 20 July 2025 / Accepted: 17 August 2025 / Published online: 18 September 2025

© The Author(s), under exclusive licence to Science Press and Institute of Geochemistry, CAS and Springer-Verlag GmbH Germany, part of Springer Nature 2025

**Abstract** The Martian core mainly contains iron, nickel and some light elements. However, controversies remain about the structure and chemical composition of the Martian core due to a lack of samples and marsquake data. Recently, the InSight lander collected long-term marsquake data, which improved the Martian interior structure model. Based on the preliminary analysis of marsquake data, Mars has a molten liquid core with a radius of around 1700 km. As the Martian core has a smaller density and lower temperature than pure iron at corresponding pressure and temperature conditions, some light elements are introduced to reduce the density and liquidus temperature. With various methods for seismic analysis, in-situ high-pressure and high-temperature experiments, and first-principal calculations, the Martian core composition and evolution models have been updated in the past few years. Here, we review those studies on the light elements in the Martian core from four aspects including (1) high-temperature and high-pressure experiments, (2) marsquake data, (3) mineral physics model with molecular dynamics simulations and (4) cosmochemistry investigation. We discussed the effect of different light elements on the Martian core's density, sound velocity and liquidus temperature. Moreover, the review examines the varieties, abundances and forms of light elements in the Martian core.

**Keywords** Martian core · Chemical composition · Iron · Light elements

✉ Shuangmeng Zhai  
zhaishuangmeng@mail.gyig.ac.cn

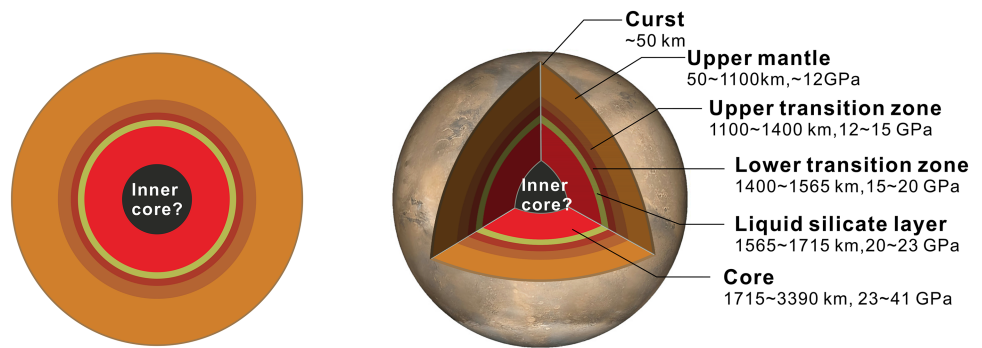
<sup>1</sup> State Key Laboratory of Critical Mineral Research and Exploration, Institute of Geochemistry, Chinese Academy of Sciences, Guiyang 550081, Guizhou, China

<sup>2</sup> University of Chinese Academy of Sciences, Beijing 100049, China

## 1 Introduction

Mars is a smaller terrestrial planet than Earth, but it may have experienced a similar early evolution to the Earth. It once had a thick atmosphere (Kite 2019; Heard and Kite 2020), significant water activity (Martín-Torres et al. 2015; Jones 2018; Nazari-Sharabian et al. 2020) and an active magnetic field (Stevenson 2001; Elkins-Tanton et al. 2003; Mittelholz et al. 2020), making it one of the planets that could potentially harbor extraterrestrial life. It is also a primary focus of current deep space exploration. After the launched InSight mission in 2018, Mars became the second extraterrestrial planet from which seismic data were obtained (Cottaar and Koelemeijer 2021; Khan et al. 2022). The preliminary analysis results on those data from InSight indicate that Mars has a large core with a radius of 1790–1870 km and a density of approximately 5.7–6.3 g/cm<sup>3</sup> (Stähler et al. 2021). Subsequent studies by Irving et al. (2023) and Le Maistre et al. (2023) slightly improved that model with a new core radius of 1780–1890 km and a density of 5.96–6.3 g/cm<sup>3</sup>, highly consistent with the results of cosmochemistry combined with geodesy (1730–1860 km) (Sohl and Spohn 1997; Rivoldini et al. 2011; Khan et al. 2018). However, recent studies have proposed a subversive model. Khan et al. (2023) and Samuel et al. (2023), by introducing a molten silicate layer at the core-mantle boundary (CMB) (Fig. 1), have reduced the radius of the Martian core to 1630–1705 km and increased the density to 6.5–6.65 g/cm<sup>3</sup>. This structure may be more consistent with the constraints of high-resolution marsquake signals. Notably, in the preliminary analysis and subsequent studies, the inversion results of InSight seismic data show that the Martian core contains many light elements. In addition, under the Martian core's pressure and temperature (P-T) conditions (~2100 K, 21–40 GPa), the core's density is approximately

**Fig. 1** The internal structure of Mars [modified from Yoshizaki and McDonough (2020)]



27% smaller than that of pure liquid iron (Khan et al. 2023). This abnormal density deficit can be explained by the mixing effects of light elements such as sulfur (S), carbon (C) and oxygen (O), which play a crucial role in understanding the formation and evolution of the Martian core and the planetary differentiation process.

Light elements have an atomic weight lower than that of liquid iron and can significantly reduce the density of the Martian core (iron-nickel) (Nishida et al. 2016; Sakamaki et al. 2016; Hirose et al. 2021). Meanwhile, light elements can lower the melting point and thermal conductivity of iron (Ohta et al. 2016; Hirose et al. 2021). This characteristic may delay the crystallization process of the core, thereby affecting the maintenance of the global magnetic field and the termination of the dynamo on Mars in its early stage (4.5–3.6 Ga) (Stevenson 2001; Mittelholz et al. 2020; Hsieh et al. 2024). On the other hand, light elements can change the sound velocity of liquid iron, thus influencing the physical

property of the core (Terasaki et al. 2019; Nishida et al. 2020; Huang et al. 2023). The Martian core has an obvious density deficit, but its sound velocity is similar to that of liquid iron (Fig. 2). Molecular dynamics results indicate that C and silicon (Si) can increase the sound velocity of liquid iron (Terasaki et al. 2019; Huang et al. 2023). However, the isotopic analysis results of SNC (Shergotty-Nakhla-Chassigny) meteorites have cast doubt on the presence of C and Si in the Martian core (Grady et al. 2004; Wood et al. 2013; Zambardi et al. 2013; Dauphas et al. 2015; Yoshizaki and McDonough 2020). Therefore, there is still no consensus on the types, contents and forms of light elements in the Martian core, as well as their impacts on the Martian core under the corresponding P-T conditions. It is shown that the existence of other light elements remains controversial except for S and O, which are recognized by most studies.

This review focuses on the investigations of the Martian core's chemical composition. We extensively collect

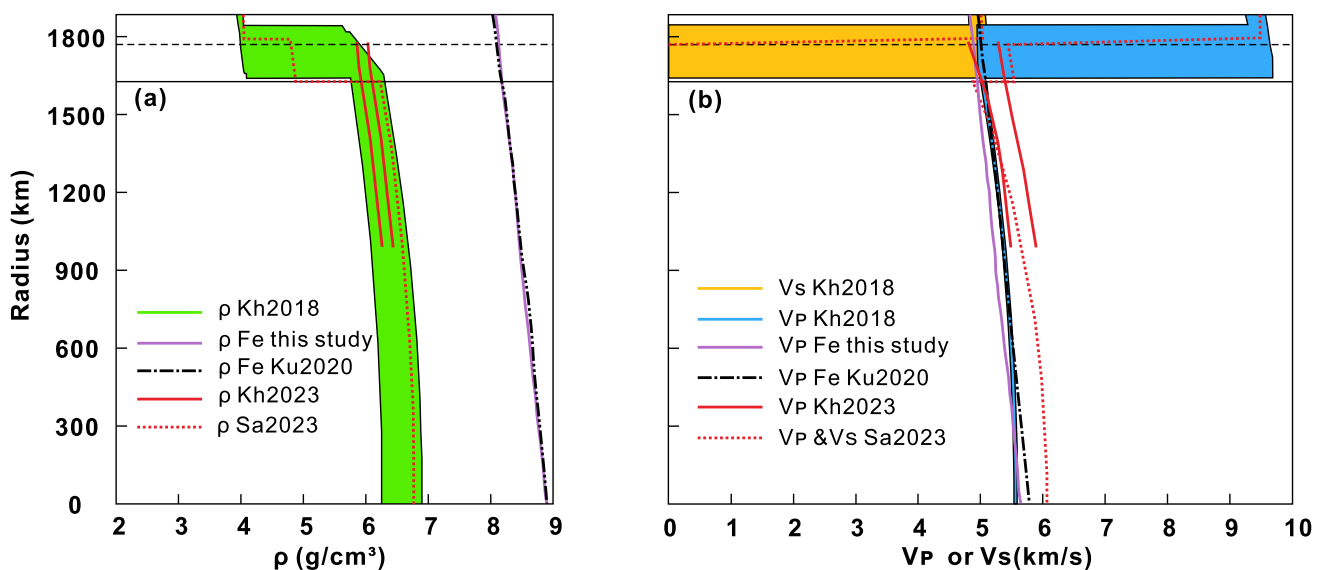


**Fig. 2** The density and sound velocity of the Martian core and pure liquid iron, where green, yellow and blue curves represent the Martian model data (Khan et al. 2018), the red curve represents the inversion results from seismic data (Khan et al. 2023; Samuel et al. 2023), the black curve represents the data for liquid Fe at 2000 K (Kuwayama et al. 2020), and the purple curve represents the liquid Fe data calculated in this study

literature and comprehensively analyze high P-T experiments, marsquake data, molecular dynamics simulations and Martian meteorite studies. This review delves into the nature, abundances and distribution of light elements in the Martian core.

## 2 Marsquake data inversion

The seismic data from Mars were collected by the InSight mission, which was launched by the US in 2018. The mission carried three main scientific instruments, i.e., the Seismic Experiment for Interior Structure (SEIS), the Heat Flow and Physical Properties Package (HP<sup>3</sup>) and the Rotation and Interior Structure Experiment (RISE) (Smrekar et al. 2019). The aim was to carry out Mars interior exploration using seismic surveys, geodesy and thermal transport, focusing on the structure and evolution of the Martian interior.

To date, the Mars Quake Service (MQS) of InSight has identified over 1000 distinct marsquake events (Clinton et al. 2021). Based on the high-quality marsquake and radio data from the InSight mission, and the geodetic data and cosmochemical models, the radius and density of the Martian core have been precisely constrained. Stähler et al. (2021) analyzed six marsquake events (S0173a, S0235b, S0407a, S0409d, S0484a, S0325a) and inverted them together with geodetic data, constraining the radius of the liquid metallic core to  $1830 \pm 40$  km and inferring an average core density of  $5.7\text{--}6.3$  g/cm<sup>3</sup>. Irving et al. (2023) observed high-quality seismic phases (secondary-kernel-secondary, SKS) passing through the Martian core in the S0976a and S1000a marsquake events, which yielded a

smaller core radius (1780–1810 km) and a larger core density ( $6.2\text{--}6.3$  g/cm<sup>3</sup>). The estimates from both Stähler et al. (2021) and Irving et al. (2023) were based on the assumption of a homogeneous Martian mantle. However, recent observations have shown abnormally slow P-wave propagation at the CMB of Mars (Khan et al. 2023) (Fig. 2), suggesting a different material composition. Samuel et al. (2021) proposed that a basal layer enriched with iron and heat-producing elements may have formed because of the early solidification of a magma ocean, potentially giving rise to a molten silicate layer above the Martian core. Samuel et al. (2023) and Khan et al. (2023) further analyzed seismic phases, providing geophysical evidence for a molten silicate layer at the top of the Martian core. Combining their findings with previous results, they recalculated the radius and density of the Martian core. Compared to earlier models, the new values suggest a smaller radius (1630–1705 km) and a larger density ( $6.50\text{--}6.66$  g/cm<sup>3</sup>) of the Martian core.

This suggests that the light elements in the Martian core include S, O, C and hydrogen (H), with the highest content of S, followed by O and C, and the lowest content of H (Stähler et al. 2021; Irving et al. 2023; Le Maistre et al. 2023), as listed in Table 1. Khan et al. (2023) found that Martian core is composed of 85–91 wt% Fe–Ni and 9–15 wt% light elements, with the light element content being lower than in other studies (16–22 wt%) (Stähler et al. 2021; Irving et al. 2023; Le Maistre et al. 2023). However, the Martian core still lacks the most crucial seismic data (Fig. 3). Therefore, determination of the structure and composition of the Martian core requires further seismic inversion and analysis with additional data in the future.

**Table 1** Varieties and abundances of light elements in Martian core

Light elements (in wt%, unless otherwise indicated)						Method	References
S	O	C	H	P	Si		
10–17	<4	<1.4	–	–	–	Mass balance calculations	Steenstra and Westrenen (2018)
18–19	<1	0.5–1.4	–	–	1.82 ppm	Theoretical calculations based on experimental parameters	Brennan et al. (2020)
6.6	5.2	–	0.9	0.33	–	Theoretical calculations based on Martian meteorites and space observation data	Yoshizaki and McDonough (2020)
10–15	<5	<1	<1	–	–	InSight Fire Seismic Data Inversion	Stähler et al. (2021)
≈9	≤2.5	≥3	≤0.5	–	–	Inverse calculations in geophysics and cosmochemistry	Khan et al. (2022)
14–19	1.3–3.5	–	–	–	≤0.07	High P-T experiments and theoretical calculations	Gendre et al. (2022)
13–17	2–3	1–2	~1	–	–	Analysis of InSight radio tracking data	Le Maistre et al. (2023)
15.4–16.5	2.9–3.2	1.2–1.4	0.5–0.6	–	–	Inversion of the SKS seismic phase by InSight	Irving et al. (2023)
7–17.6	0.3–1.9	0.4–1.7	–	–	–	High-pressure melting experiment	Yokoo and Hirose (2024)

Means that the absence or low level is not specified

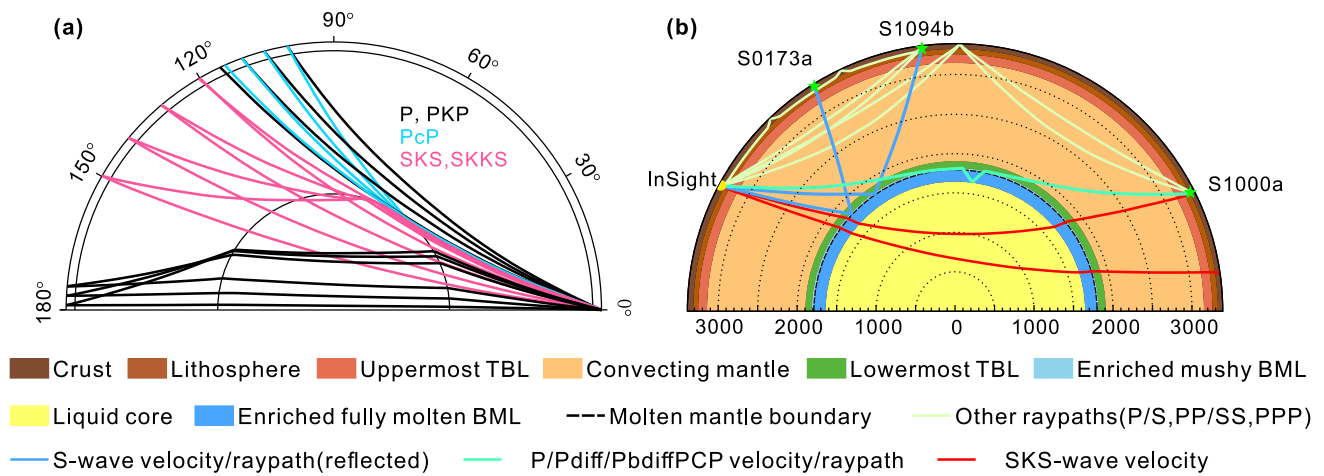


**Fig. 3** **a** The seismic wave ray paths of the model without a solid inner core proposed by Sohl and Spohn (1997) [modified according to Helffrich (2017)]. **b** The ray paths of the marsquake data from the InSight mission, where TBL is the thermal boundary layer and BML is the basal mantle layer [modified according to Samuel et al. (2023)]

### 3 Iron-light element system

High P-T experiments are widely applied in the deep exploration of the Earth and play a crucial role in the research on the mantle and core. Fe-light element phase diagrams under high P-T conditions are important for understanding the elemental composition and solid-liquid phase characteristics of planetary core (Komabayashi 2021; Li and Fei 2014). The results of Fe-light element systems carried out corresponding to the conditions of the Martian core are summarized in Table 2. The phase diagrams mainly focus on binary systems (Fe–S) and ternary systems (Fe–S–O, Fe–S–H, Fe–Ni–S, Fe–Ni–Si),

with two studies on quaternary systems (Fe–Ni–S–C, Fe–S–O–C); studies of more complex systems are still relatively lacking.

#### 3.1 Fe–S and Fe–Ni–S systems

It is believed that the Martian core is dominated by Fe, Ni and some light elements. S is considered the primary light element in the Martian core. Therefore, the Fe–S and Fe–Ni–S systems have been widely investigated. If S is the only light element in the Martian core, 30 wt% sulfur would be required (Terasaki et al. 2019; Stähler et al. 2021) to match the density profile, which exceeds the upper limit of cosmochemical estimates (18–19%)

**Table 2** Results of Fe-light element systems under Martian core conditions

System	Experimental conditions	Results	References
Fe–Ni–S	23–40 GPa, 1400–2000 K	14.2 wt% S	Fei and Bertka (2005)
Fe–Ni–S	18–52 GPa, 1275–2300 K	The core of Mars is believed to be liquid	Fei et al. (2006)
Fe–S, Fe–Ni–S	23–40 GPa, 1113–1973 K	12–16 wt% S	Stewart et al. (2007)
Fe–Ni–S	19–23 GPa, 1073–1373 K	Ni significantly increases the solubility of S	Zhang and Fei (2008)
Fe–Ni–S–C	6–13 GPa, 2073–2273 K	10–16 wt% S, 0.25–0.9 wt% C	Tsuno et al. (2018)
Fe–S, Fe–S–O	14–20 GPa, 1673–2123 K	O has almost no effect on the liquidus temperature	Pommier et al. (2018)
Fe–Ni–Si, Fe–Ni–S	0–13 GPa, 1240–2250 K	32.4 wt% S or 30.3 wt% Si	Terasaki et al. (2019)
Fe–S	5–20 GPa, 1700–2300 K	S has almost no effect on the $V_p$ of liquid Fe	Nishida et al. (2020)
Fe–S, Fe–Ni–S	20 GPa, 1473–2073 K	The lower boundary of the CMB temperature for a fully molten core is defined as 1250–1500 K	Gilfoy and Li (2020)
Fe–S–H	23–45 GPa, 1150–4579 K	A new phase of $\text{FeS}_x\text{H}_y$ was discovered at 36 GPa, where $x \approx 1$ and $y \approx 1$	Piet et al. (2021)
Fe–S–O	2–12 GPa, 1673–2473 K	14–19 wt% S, 1.3–3.5 wt% O	Gendre et al. (2022)
Fe–S–O–C	26–49 GPa, 1270–2510 K	7.0–17.6 wt% S, 0.3–1.9 wt% O, 0.4–1.7 wt% C	Yokoo and Hirose (2024)

(Steenstra and van Westrenen 2018; Brennan et al. 2020). In the Fe-S system, S can significantly lower the melting temperature of Fe (Fig. 4). The addition of Ni slightly changes the liquidus and lowers the eutectic temperature (Stewart et al. 2007) but increases the solubility of sulfur in liquid Fe (Zhang and Fei 2008). Moreover, S can significantly reduce the sound velocity and bulk modulus of liquid Fe (Terasaki et al. 2019). However, the experimental study by Nishida et al. (2020) shows that under pressure conditions close to those of the Martian core ( $\sim 40$  GPa), the weakening effect of sulfur on the sound velocity of liquid iron gradually weakens and eventually becomes negligible (Fig. 5). In contrast, Huang et al. (2023) systematically calculated the quantitative effects of S molar concentration on the sound velocity and density of liquid Fe through ab initio molecular dynamics simulations. The results show that the density of liquid Fe has a significant negative correlation with the S concentration under the conditions of both 19 GPa/2100 K and 35 GPa/2400 K (Fig. 6a). However, the influence of the S concentration on the sound velocity of liquid Fe exhibits pressure dependence. As the pressure condition increases, the influence of S on the sound velocity of liquid Fe gradually weakens (Fig. 6b). The simulation results of Huang et al. (2023) share certain commonalities with the experimental results of Nishida et al. (2020), but there are still significant differences. Although the simulation by Huang et al. (2023)

incorporated the influence of magnetic effects on the equation of state (EOS) of iron-rich liquids, it has not yet fully bridged the gap between first-principles molecular dynamics simulations and high P-T experimental results. The latest research by Liu and Jing (2025) shows that the results obtained by adopting component-dependent pressure correction are more consistent with the experimental results than the constant pressure correction results used by Huang et al. (2023). This composition dependence was largely ignored in earlier studies. However, the impact of other light elements on pressure correction remains unclear, and further investigations are required.

Yoshizaki and McDonough (2020) proposed that the S content in the Martian core is 6.6 wt% based on cosmochemical models. However, high P-T experiments show that the solubility of S in iron alloy is relatively high, ranging from 7 wt% to 19 wt% (Gendre et al. 2022; Yokoo and Hirose 2024), which is closer to the inversion results of InSight (10–16.5 wt% S) (Stähler et al. 2021; Irving et al. 2023; Le Maistre et al. 2023). Man et al. (2025) further studied the Fe-S system and suggested that when the S content is 18–22 wt%, a solid Martian inner core with a composition of  $\text{Fe}_{4+x}\text{S}_3$  may form. Although the S content range in the study of Man et al. (2025) exceeds the upper limit estimated by cosmochemistry, it provides certain references for subsequent multi-system research and the state of the Martian core.

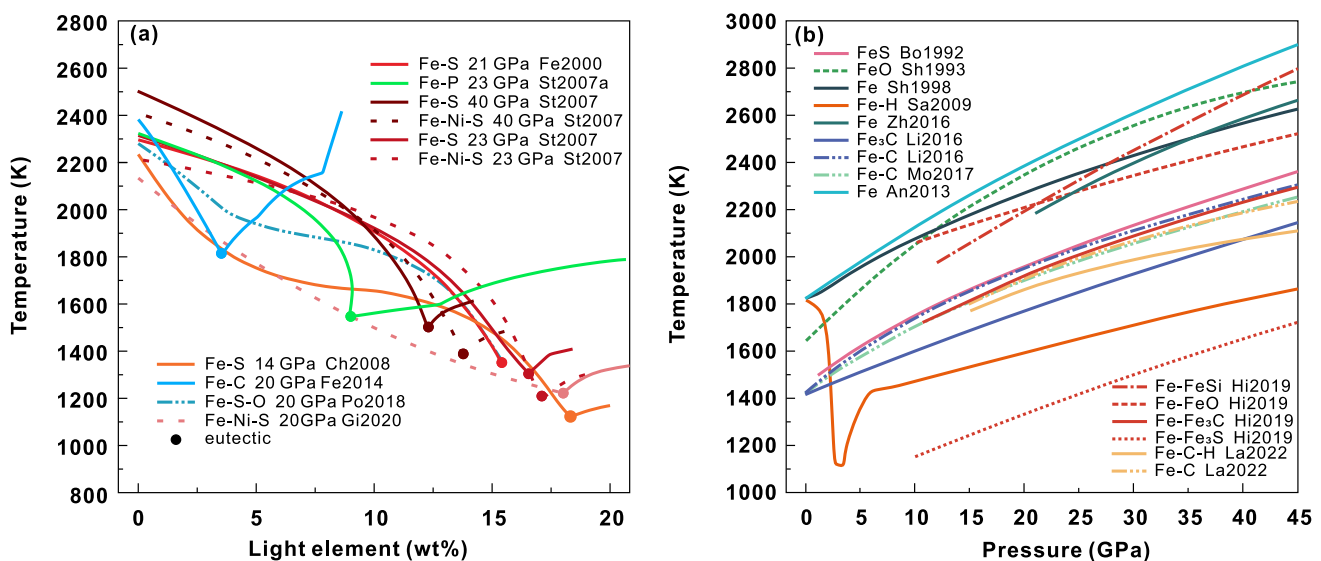


**Fig. 4** **a** Liquidus curve and eutectic points of the Fe-light element system, where the S content is used as the x axis in the Fe-S-O system. **b** High-pressure melting curves of the Fe-light element system and Fe alloys. References: Bo1992 = Boehler (1992); Sh1993 = Shen et al. (1993); She1998 = Shen et al. (1998); Fe2000 = Fei et al. (2000); Ch2008 = Chen et al. (2008); St2007a = Stewart and Schmidt (2007); St2007 = Stewart et al. (2007); Sa2009 = Sakamaki et al. (2009); Fe2014 = Fei and Brosh (2014); Zh2016 = Zhang et al. (2016); Li2016 = Liu et al. (2016); Mo2017 = Morard et al. (2017); Pr2018 = Prommier et al. (2018); An2013 = Anzellini et al. (2013); Hi2019 = Hirose et al. (2019); Gi2020 = Gilfooy (2020); La2022 = Lai et al. (2022)

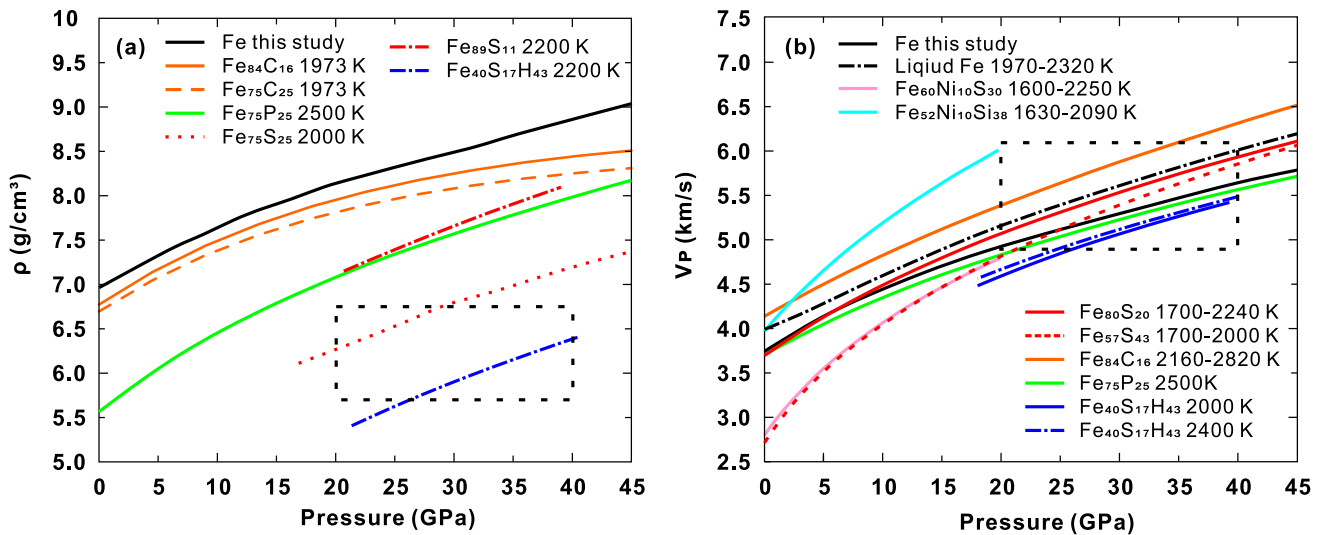


**Fig. 5** The curves of the density (a) and sound velocity (b) of Fe-light elements under Martian pressures. The position of the dashed-line box represents the range of Martian core density and sound velocity obtained from the inversion of InSight marsquake data (Irving et al. 2023; Samuel et al. 2023). The Fe–C data are from Nakajima et al. (2015) (the density data after 10 GPa were obtained by extrapolating the data from this reference); the Fe–P data are from Kinoshita et al. (2020); the data for Fe<sub>89</sub>S<sub>11</sub> and Fe<sub>40</sub>S<sub>17</sub>H<sub>43</sub> are from Liu and Jing (2025); the data for Fe<sub>75</sub>S<sub>25</sub> are from Li et al. (2024b); the data for Fe<sub>80</sub>S<sub>20</sub>, Fe<sub>57</sub>S<sub>43</sub> and liquid Fe are from Nishida et al. (2020); the data for Fe–Ni–S and Fe–Ni–Si are from Terasaki et al. (2019)

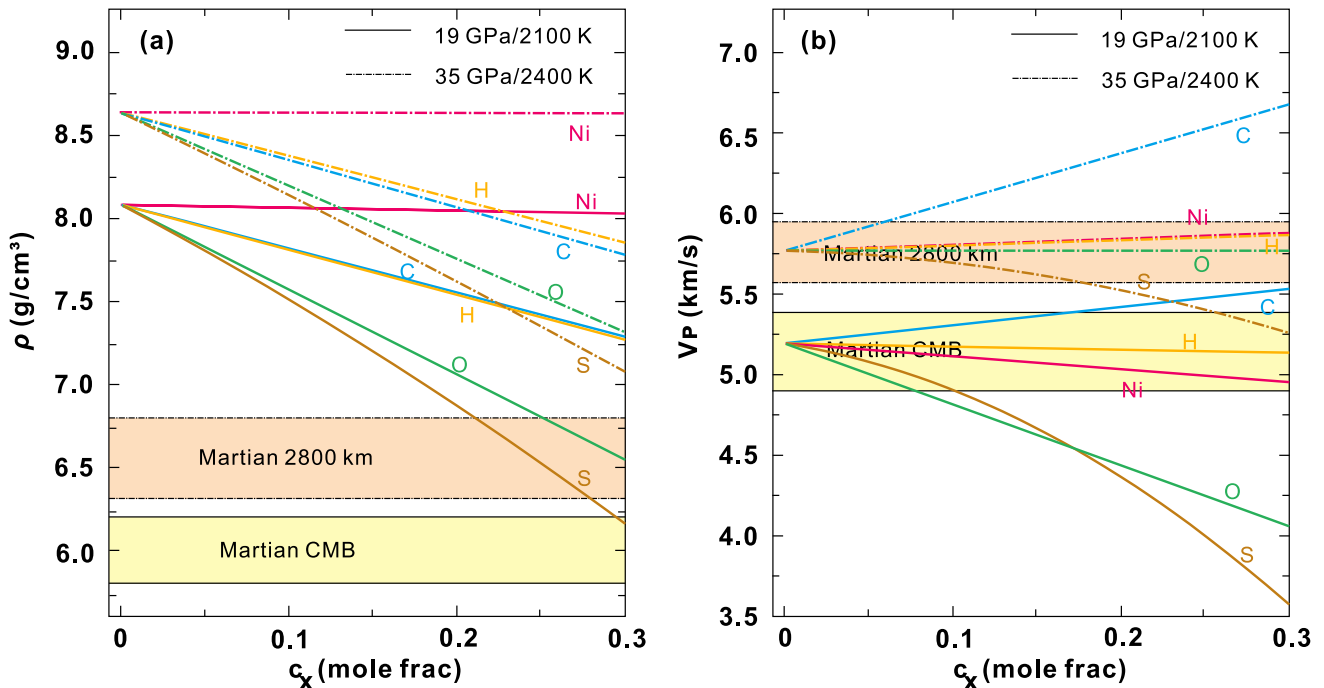


**Fig. 6** The effect of light elements X (X=Ni, S, C, O and H) at the CMB and at a depth of 2800 km on the density and sound velocity of liquid Fe (modified from Huang et al. (2023), where the range of  $V_p$  is referenced from Mars models and seismic wave detection results)

### 3.2 Fe–Ni–Si systems

Hirose et al. (2019) showed that the melting curves of Fe–FeSi were similar to those of Fe (Shen et al. 1998; Zhang

et al. 2016) (Fig. 4b), which proves that Si basically has a small effect on the liquidus of Fe. If the silicon content in the core is relatively high, a solid inner core may form under the current P–T conditions of the Martian core. However, Si

is a lithophile element and only exhibits siderophile properties at low oxygen fugacity (IW-4.5) (Fischer et al. 2015). The relatively high oxygen fugacity (IW-2 to -1) during the formation of the Martian core (Yoshizaki and McDonough 2020) limits the siderophile nature of Si. Besides, through cosmochemical analysis, Zambardi et al. (2013) and Dauphas et al. (2015) found that no Si isotopic fractionation was caused by metal-silicate separation in Martian meteorites. This evidence points to an extremely low content or even the absence of Si in the Martian core.

By using first-principles molecular dynamics simulations, Umemoto and Hirose (2020) calculated the ability of light elements to reduce the density of liquid Fe. Their results showed an order of  $\text{Si} > \text{S} > \text{O} > \text{C} \approx \text{H}$ , indicating that Si has the greatest ability to reduce the density of liquid Fe due to the substitutional doping. Moreover, the bulk modulus of liquid Fe remains constant with Si content (Terasaki et al. 2019). Thus, the sound velocity of Si-rich liquid Fe is higher than that of pure liquid Fe and S-rich liquid Fe (Fig. 5) (Terasaki et al. 2019; Yamada et al. 2023). Meanwhile, at 300 K, the incorporation of Si increases the  $V_p$  of body-centered cubic (bcc) Fe by 0.074(15) km/s (Li et al. 2024a). Early Martian core models and recent SKS seismic wave data from InSight show that the sound velocity in the Martian core is similar to that of pure liquid Fe, and even slightly higher than that of pure liquid Fe (Fig. 2). Based on the equation of state for liquid Fe proposed by Kuwayama et al. (2020), we calculated the density and sound velocity of liquid Fe under Martian core conditions. Under the CMB condition, the calculated sound velocity of liquid Fe is 4.9–5.1 km/s, slightly lower than the seismic wave results (4.9–5.5 km/s) (Irving et al. 2023; Samuel et al. 2023). Other light elements (S, O and H) reduce the sound velocity of liquid Fe (Huang et al. 2023), providing the possibility of the presence of Si in the Martian core.

### 3.3 Fe–H and Fe–S–H systems

H is abundant in the solar system. It is lithophile under low temperatures and low pressures, but becomes siderophile under high pressures (20–30 GPa) (Oka et al. 2022). Suzuki et al. (1984) found that the melting temperature of the Fe–H system at about 5.4 GPa was  $\sim 500$  K lower than that of pure iron, demonstrating that H effectively lowers the melting point of pure iron. Recently, Yuan and Steinle-Neumann (2023) showed that the melting point of Fe decreases by 700–900 K for 0.34% H at 330 GPa. Figure 4b shows that the liquidus of the H-containing system is significantly lower than those of the other systems.

In the Fe–S–H system, the addition of H leads to the emergence of a new phase containing both S and H ( $\text{FeS}_x\text{H}_y$ , where  $x \approx 1$  and  $y \approx 1$ ), and it also affects the stability of  $\text{Fe}_3\text{S}$  (Piet et al. 2021; Wei et al. 2024). Influenced by pressure,

$\text{FeS}_x\text{H}_y$  appears when the pressure is  $> 35$  GPa, while Fe–H and Fe–S alloys appear separately at 23–35 GPa (Piet et al. 2021). In addition, Wei et al. (2024) studied the effect of H content on the Fe–S system at 30–40 GPa. Their research shows that when the H content is low ( $\leq 0.06$  wt%), the  $\text{Fe}_3\text{S}$  phase is stable; when there is low S and high H ( $\text{H} \geq 0.14$  wt% and  $\text{S} \leq 16$  wt%), Fe–H and Fe–S alloys coexist; when the H content is too high ( $\geq 0.33$  wt%),  $\text{FeS}_x\text{H}_y$  appears. The preliminary inversion results of InSight seismic data and the analysis of Martian meteorites show that the H content is 0.5–1 wt% (Yoshizaki and McDonough 2020; Stähler et al. 2021; Khan et al. 2022; Le Maistre et al. 2023; Irving et al. 2023), and further research by Khan et al. (2023) suggests that the H content in the Martian core can be up to 2 wt%. Therefore, based on current studies of H content in the Martian core, it is difficult for the  $\text{Fe}_3\text{S}$  phase to exist stably, and the  $\text{FeS}_x\text{H}_y$  phase is more likely to form there. The ab initio molecular dynamics show that H can reduce the density of liquid iron, but its effect on the sound velocity is not obvious (Huang et al. 2023) (Fig. 6). Liu and Jing (2025) obtained similar results using first-principles molecular dynamics simulations. They also calculated that the density of the Fe–S–H system can match that of the Martian core, but the corresponding sound velocity is always slightly lower than the P-wave velocity observed from Martian seismic data. Therefore, the presence of C or Si in the core is necessary to increase the sound velocity.

### 3.4 Fe–S and Fe–P–S systems

Iron phosphides are widely found in meteorites (Skála and Čisářová 2005; Chantel et al. 2018). Therefore, phosphorus (P) is considered one of the candidate light elements in planetary cores. P is a moderate siderophile element and becomes more siderophile under reducing conditions (Newsom and Drake 1983). The Martian surface soil is rich in P (Greenwood and Blake 2006), and the P content in the Martian mantle is approximately 5–10 times that of the Earth's mantle (Gellert et al. 2006; Ming et al. 2008; Gu et al. 2019). Furthermore, P has a high partition coefficient between liquid silicates and liquid metals, suggesting that a significant amount of P could be incorporated into the Martian core (Gu et al. 2019). Stewart and Schmidt (2007) studied the Fe–P–S system at 23 GPa. Compared to the Fe–S system in Stewart et al. (2007), the eutectic point temperature of the Fe–P system is higher than that of the Fe–S system (Fig. 4a). The liquidus of the Fe–P system shows different trends with the content of light elements. When the content of light elements is low ( $< 14$  wt%), the liquidus temperature of the Fe–P system is lower than that of the Fe–S system, and vice versa, it is higher than that of the Fe–S system (Fig. 4a). Chantel et al. (2018) studied the Fe–P system under low pressure (2–7 GPa) and found that the

liquidus temperature of the Fe–P system exhibits a bimodal characteristic regarding composition: for P-poor components (Fe-5 wt% P), the liquidus has a positive correlation with pressure, while for P-rich components (Fe-10 wt% P), it has a negative correlation. Moreover, they believe that this compositional dependence implies that the P content can regulate the crystallization direction of the core. However, due to the relatively low-pressure conditions in this study, it remains unclear whether such a pattern still holds under the pressure conditions of the Martian core. More research data are needed in the future to support this.

Based on the cosmochemical analysis of Martian meteorites by Yoshizaki and McDonough (2020), the P content of the Martian core is constrained to be approximately 0.33 wt%. When combined with the research results of Chantel et al. (2018), the Martian core is more inclined to the crystallization mechanism of the "snowing-core model", that is, light elements gradually crystallize from the top to the bottom of the core along with the iron alloy melt. Further comparing the density-pressure curves of the Fe–P, Fe–S and Fe–C systems in Fig. 5a (with the atomic proportion of light elements in each system being 25%) shows that the effect of P on reducing the density of liquid iron is between that of S and C (i.e.,  $\rho\text{-P} > \rho\text{-C}$  but  $\rho\text{-P} < \rho\text{-S}$ ), indicating that P plays a medium-strength role in regulating the density deficit of the planetary core. However, high P-T experiments by Kinoshita et al. (2020) show that although P significantly reduces the density of liquid iron, its effect on the sound velocity is relatively weak (Fig. 5b). This is because while P reduces the density, it simultaneously decreases the bulk modulus ( $K_s$ ), resulting in a partial cancellation of their contributions to the sound velocity ( $V_p = \sqrt{\frac{K_s}{\rho}}$ ). Notably, current experimental studies on phosphorus-containing ternary systems under planetary core conditions are still extremely limited, and there is a severe shortage of phase equilibrium and physical property data for complex multi-component systems. This greatly restricts the quantitative analysis of the mechanisms of core-mantle differentiation and planetary magnetic field evolution by light elements.

### 3.5 Fe–S–O and Fe–S–O–C systems

Both O and C can reduce the density of liquid iron. It is believed that O has an inhibitory effect on the sound velocity of liquid Fe, while C, like Si, can increase the sound velocity of liquid Fe (Huang et al. 2023). Previous studies have shown that the solubility of O in liquid Fe is positively correlated with P-T conditions (Ohtani et al. 1984; Siebert et al. 2013; Badro et al. 2015). The solubility of O in liquid iron is only 0.74 wt% under the conditions of 21 GPa and 2573 K (Ricolleau et al. 2011). However, the sulfur in liquid iron can lower the P-T conditions for oxygen to dissolve in

liquid iron (Tsuno et al. 2011). Due to the promoting effect of sulfur, the content of oxygen in the Martian core is relatively high (0.3–3.5 wt%) (Gendre et al. 2022; Yokoo and Hirose 2024). Pommier et al. (2018) conducted experiments on the Fe–S–O system at 14 GPa and 20 GPa with temperatures up to 2123 K and found that oxygen has little effect on the liquidus temperature compared to the Fe–S system (Fig. 4). However, the addition of oxygen causes the formation of solid FeO phase in the system, stable between 1673 and 2033 K, providing a potential scenario for the existence of a solid inner core on Mars.

Early studies do not support the presence of C in the Martian core. On the one hand, Martian meteorites lack the C isotopic fractionation similar to that in terrestrial rocks (Grady et al. 2004; Wood et al. 2013), which weakens the possibility of the presence of C in the Martian core. On the other hand, there is a significant difference between the actual density of the Martian core and that of liquid iron, while C has little effect on the density of liquid Fe and thus cannot effectively reduce the density of the Martian core (Nakajima et al. 2015; Yoshizaki and McDonough 2020). Therefore, C is excluded as a candidate for light elements in the Martian core. However, C is a siderophile element and has a greater tendency to enter the metallic core during the core-mantle differentiation process (Chi et al. 2014; Li et al. 2015, 2016). Moreover, C can increase the sound velocity of liquid iron alloys (Figs. 5b and 6b) (Nakajima et al. 2015; Huang et al. 2023), which is consistent with the fact that the P-wave sound velocity of the Martian core revealed by the inversion of InSight marsquake data is higher than that of liquid iron (Fig. 2b) (Irving et al. 2023; Samuel et al. 2023). In addition, the results of multiple recent studies show that there may be 0.4–3 wt% C in the Martian core (Steenstra and Westrenen 2018; Brennan et al. 2020; Stähler et al. 2021; Khan et al. 2022; Le Maistre et al. 2023; Irving et al. 2023; Yokoo and Hirose 2024), which further provides supporting data for the presence of C in the Martian core. In the Fe–S–O–C system, the solubility of C in the liquid alloy decreases with increasing S content. When the S content is < 9 wt%, the crystallization of an FeO inner core or a mixed FeO + Fe<sub>3</sub>C inner core will form (Yokoo and Hirose 2024), providing a reference for the composition and existence of the solid inner core of Mars.

Based on the current research progress, high P-T experiments on the phase diagram analysis of the Fe-light element system initially revealed the influence laws of single elements on the liquidus line and the eutectic point temperature: S, H and P can effectively lower the liquidus line of Fe, while O and Si have almost no effect on the temperature of the liquidus line, and the eutectic point temperature of C is relatively high (Fig. 4). Accordingly, it is inferred that O and C may play a key role in the formation of the solid inner core of Mars, while Si is not considered here because of the

major current controversy. In addition, the influence of light elements on the density and sound velocity of liquid iron obtained from high P-T experiments and molecular dynamics simulations, after cross-validation with the core physical property parameters inverted from the seismic observation data of InSight, has determined the necessity of the element C (and/or Si) in the composition of the Martian core.

## 4 Discussion

### 4.1 State of the Martian core

Fei and Bertka (2005) summarized the evidence from three aspects—the Martian magnetic field (Acuña et al. 1999; Connerney et al. 1999), solar tidal deformation of Mars (Stevenson 2001) and high P-T experiments (Fei et al. 2000)—and proposed that the Martian core may be completely liquid. Then, different researchers have studied the state of the Martian core through geodesy, geophysics and high P-T experiments (Stewart et al. 2007; Rivoldini et al. 2011; Khan et al. 2018; Yokoo and Hirose 2024). Most of the studies suggest that Mars has a liquid core, but there is no definitive conclusion.

Based on the no-solid-inner-core model from Sohl and Spohn (1997), Helffrich (2017) predicted the seismic wave ray paths that might be obtained by the InSight mission for a core without a solid inner core (Fig. 3a). However, seismic wave ray paths that directly pass through the deepest core

of Mars are lacking (Fig. 3b). Recently, Bi et al. (2025) analyzed the seismic data from the InSight mission and identified two key phases indicating of the presence of a solid inner core in the S0235b seismic event, namely the deep core-crossing phase PKKP and the core-mantle boundary reflection phase PKiKP (Fig. 7). They suggest a solid Martian inner core with a radius of  $600 \pm 50$  km (Bi et al. 2025), making it the first study to infer the existence of a Martian inner core based on the inversion of InSight seismic data. High P-T experiments have predicted the possible compositions of the solid inner core:  $\text{Fe}_{4+x}\text{S}_3$ , FeO and  $\text{Fe}_3\text{C}$  (Yokoo and Hirose. 2024; Man et al. 2025). However, whether Mars has a completely liquid core or a liquid outer core and a solid inner core, the Martian dynamo is an inevitable issue. The way the liquid core generates a magnetic field depends on thermal convection (Stevenson 2001; Fei et al. 2006). High thermal conductivity promotes efficient cooling of the Martian core and the formation of a thermally stratified structure, resulting in the short-term maintenance of its magnetic field dynamo activity. For planets with a solid inner core, the dynamo is maintained through compositional convection, and in this case, the dynamo is generally stable over the long term (Stevenson 2001). If there is a solid inner core in the Martian core, how should we explain the current absence of a global magnetic field on Mars? Hemingway and Driscoll (2021) suggest that the existence of a solid inner core on Mars is not in conflict with the current lack of a global magnetic field. Bi et al. (2025) also believe that the process of gradual crystallization of the Martian core is

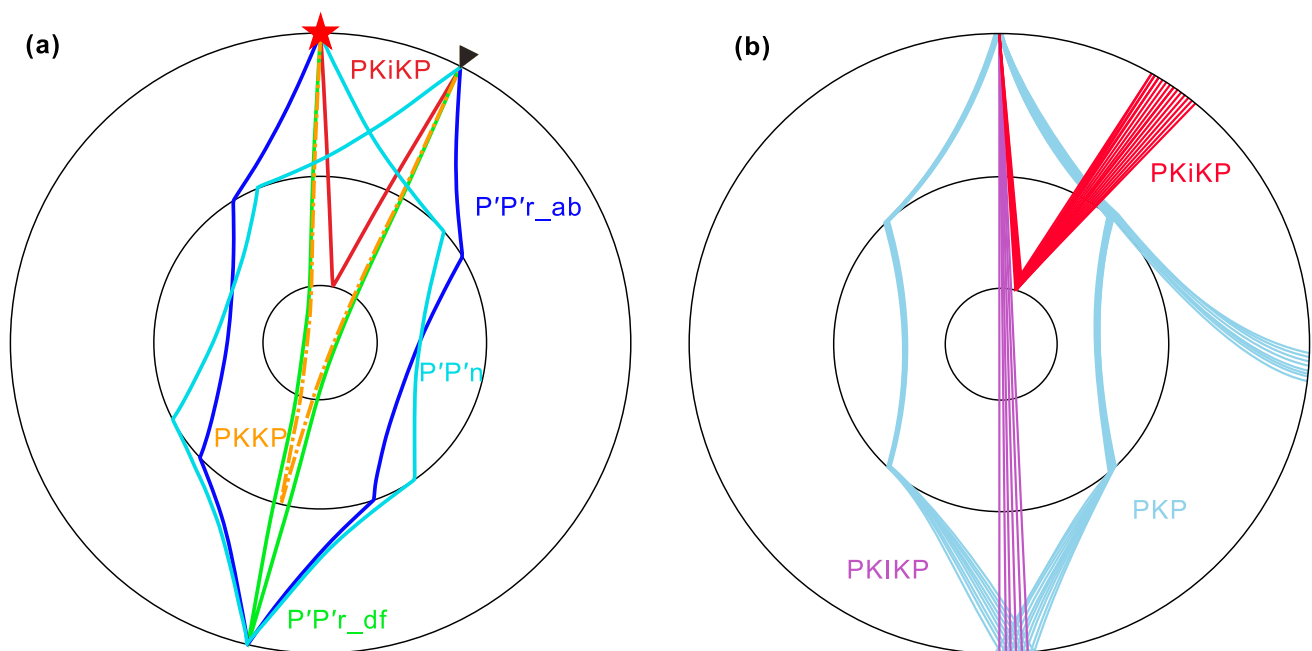


**Fig. 7** Ray paths of seismic waves in the Martian core with a solid inner core [modified from Bi et al. (2025)]. The red star represents a Mars seismic event at a depth of 33 km, and the black triangle represents the InSight seismometer

not necessarily inconsistent with the current situation where there is no dynamo on Mars.

## 4.2 Partitioning behavior of light elements

Planetary core-mantle differentiation is a key process that shapes the internal structure and evolutionary paths of terrestrial planets. The core-mantle differentiation process of Mars may have occurred under the conditions of 10–22 GPa, 1900–2300 K and an oxygen fugacity of IW-2 to -1 (Righter and Chabot 2011; Rai and van Westrenen 2013; Yoshizaki and McDonough 2020; Li et al. 2025). However, under the extreme physical and chemical conditions during the formation of Mars, the partitioning behavior of light elements during core-mantle differentiation is difficult to directly observe. High P-T experiments have become a core means to analyze this process.

High P-T experiments accurately reproduce the pressure and temperature conditions of the Martian magma ocean stage through multi-anvil high-pressure devices (Tsuno et al. 2018; Pommier et al. 2018; Terasaki et al. 2019; Nishida et al. 2020; Gilfooy and Li 2020), laser-heated diamond anvil cells (LH-DAC) (Fei et al. 2006; Piet et al. 2021; Yokoo and Hirose 2024) and sintered diamond secondary presses (Stewart et al. 2007). Finally, techniques such as electron probe microanalysis and secondary ion mass spectrometry (SIMS) are used to determine the elemental concentrations in the two phases and calculate the partition coefficients.

The significant density deficit of the Martian core suggests that it contains light elements such as S, O, C, H, P and Si. As the light element with the highest abundance in the Martian core, S exhibits siderophile under the conditions of Martian core formation and is not sensitive to the changes in temperature and pressure during core formation (Steenstra and van Westrenen 2018). The partition coefficient of O under the conditions of the Martian core is low and decreases with the decreasing pressure and temperature (Ohtani et al. 1984; Ricolleau et al. 2011; Siebert et al. 2013; Badro et al. 2015). However, the high P-T experiment on the Fe–S–O system shows that oxygen solubility in the metal increases as increasing sulfur content, suggesting high oxygen abundance in the Martian core (Tsuno et al. 2011; Gendre et al. 2022; Yokoo and Hirose 2024). The partition coefficient of Si between the metal and silicate is low and has stronger temperature dependence compared with pressure (Fischer et al. 2015). Carbon is siderophile under the P-T conditions of Martian core-mantle differentiation (Chi et al. 2014; Li et al. 2015, 2016). In the Fe–S–C system, the partition behavior of carbon is inhibited by the sulfur content, further limiting the content of carbon (Tsuno et al. 2018; Yokoo and Hirose 2024). Moreover, Si and H also have inhibitory effects on C to varying degrees (Li et al. 2015; Takahashi et al. 2013; Hirose et al. 2019). It is difficult

for H to be incorporated into the Martian core under its pressure conditions (Ricolleau et al. 2011; Siebert et al. 2013; Badro et al. 2015; Clesi et al. 2018), but the ringwoodite at the CMB of Mars facilitates the entry of H (Shibazaki et al. 2009). Gu et al. (2019) showed that the partition coefficient of P between liquid metal and silicate increases with the increase of pressure and decreases with the increase of temperature, and it decreases with increasing sulfur content (Siebert et al. 2011). High P-T experiments provide key parameters for constraining the evolutionary model of the Martian core and mantle by quantifying the partitioning behavior of elements. In the future, with the development of synchrotron radiation in situ observation, we will be able to more accurately constrain the details of Martian core-mantle differentiation, thereby laying a more solid scientific foundation for understanding the commonalities in the formation of terrestrial planets and the unique evolutionary path of Mars.

## 5 Conclusion and outlook

In this review of light elements in the Martian core, we focus on the effects of light elements on liquid Fe, aiming to clarify the varieties and abundances of light elements in the Martian core. The results of the density and sound velocity of the Martian core obtained by inverting the Martian meteorite models and marsquake data were considered. After comprehensively analyzing the effects of light elements on the density, sound velocity and liquidus of liquid iron, the main light element components in the Martian core include S, O, C and H. In addition, Si and P are also possible in the core. Further works are needed to verify and supplement the specific existence and roles of these light elements in the Martian core.

Current research faces challenges such as insufficient precision in high P-T experiments, limited resolution of seismic data, bottlenecks in simulation methods and constraints in cosmochemical analysis. Breakthroughs in these bottlenecks require interdisciplinary technological innovations.

Regarding high P-T experiments, measuring the physical properties of liquid iron-light element systems is critically difficult. In situ observation of liquid samples is restricted by signal interference and sample stability under high-temperature and high-pressure conditions. The precision of existing technologies is prone to being affected by temperature gradients and pressure fluctuations. In the future, it will be necessary to develop in situ dynamic x-ray scattering technology based on synchrotron radiation light sources, combined with diamond anvil cells (DAC) and/or large volume press, to achieve real-time high-precision measurement of electrical conductivity, viscosity and sound velocity of liquid iron alloys. Observed seismic data are an important basis for inverting the physical state of the Martian core. However, the data from the existing

InSight mission are still insufficient to clearly determine the composition of the Martian core, and future missions will be needed to further reduce the uncertainty about its composition. Molecular dynamics simulations need to overcome the limitations of existing potential functions. Meanwhile, developing a dynamic pressure correction model coupled with composition, temperature and pressure can more accurately describe the thermodynamic behavior of liquid iron alloys under core conditions, providing theoretical support for integrating high P-T experimental results and seismic observations. In cosmochemical research, traditional Martian meteorite analysis is limited by the crust-mantle origin of samples, making it difficult to directly constrain core composition. In the future, high P-T experiments can be combined with trace element analysis of meteorites: by simulating core-mantle differentiation conditions, measuring the partition coefficients of siderophile elements between liquid iron and silicate melts and combining them with isotopic anomalies in meteorites, the content of light elements during core formation can be inferred.

In summary, through technical developments in high P-T experiments, deployment of Martian seismic networks, optimization of simulation methods and interdisciplinary data integration, it is expected that the precision of constraining the composition of the Martian core will be largely improved in the next decade, providing breakthrough empirical evidence for the construction of theories on the evolution of terrestrial planets.

**Acknowledgements** The authors thank Dr. Yuan Yin for his helpful discussion and suggestion. Helpful comments and suggestion from an anonymous reviewer and Prof. Yuan Li are grateful. This work was financially supported by the National Natural Science Foundation of China (grant no. 42120104005), Guizhou Provincial 2021 Science and Technology Subsidies (grant no. GZ2021SIG) and Guizhou Provincial Science and Technology Projects (grant nos. ZK[2024]087; GCC[2023]060).

**Author contributions** Yinfang Yang: collecting data, drawing figures, writing manuscript; Shuangmeng Zhai: Conceptualization, providing modification suggestion, polishing the manuscript, funding support.

**Data availability** All data supporting the conclusions of this paper can be found in the cited references, tables.

#### Declarations

**Conflict of interest** The authors declare that they have no conflict of interest.

## References

- Acuña MH, Connerney JEP, Ness NF, Lin RP, Mitchell D, Carlson CW, McFadden J, Anderson KA, Rème H, Mazelle C, Vignes D, Wasilewski P, Cloutier P (1999) Global distribution of crustal magnetization discovered by the Mars global surveyor MAG/ER experiment. *Science* 284(5415):790–793. <https://doi.org/10.1126/science.284.5415.7>
- Anzellini S, Dewaele A, Mezouar M, Loubeyre P, Morard G (2013) Melting of iron at Earth's inner core boundary based on fast x-ray diffraction. *Science* 340(6131):464–466. <https://doi.org/10.1126/science.1233514>
- Badro J, Brodholt JP, Piet H, Siebert J, Ryerson FJ (2015) Core formation and core composition from coupled geochemical and geophysical constraints. *Proc Natl Acad Sci USA* 112(40):12310–12314. <https://doi.org/10.1073/pnas.1505672112>
- Bi X, Sun D, X, Sun N, Mao Z, Dai M, Hemingway D (2025) Seismic detection of a 600-km solid inner core in Mars. *Nature* 645:67–72. <https://doi.org/10.1038/s41586-025-09361-9>
- Boehler R (1992) Melting of the Fe-FeO and the Fe-FeS systems at high pressure: Constraints on core temperatures. *Earth Planet Sci Lett* 111:217–227. [https://doi.org/10.1016/0012-821X\(92\)90180-4](https://doi.org/10.1016/0012-821X(92)90180-4)
- Brennan MC, Fischer RA, Irving JCE (2020) Core formation and geophysical properties of Mars. *Earth Planet Sci Lett* 530:115923. <https://doi.org/10.1016/j.epsl.2019.115923>
- Chantel J, Jing ZC, Xu M, Yu T, Wang YB (2018) Pressure dependence of the liquidus and solidus temperatures in the Fe-P binary system determined by *in situ* ultrasonics: implications for the solidification of Fe-P liquids in planetary cores. *J Geophys Res Planets* 123(5):1113–1124. <https://doi.org/10.1029/2017JE005376>
- Chen B, Gao L, Leinenweber K, Wang YB, Sanehira T, Li J (2008) *In-situ* investigation of high-pressure melting behavior in the Fe-S system using synchrotron X-ray radiography. *High Press Res* 28:315–326. <https://doi.org/10.1080/08957950802318883>
- Chi H, Dasgupta R, Duncan MS, Shimizu N (2014) Partitioning of carbon between Fe-rich alloy melt and silicate melt in a magma ocean—implications for the abundance and origin of volatiles in Earth, Mars, and the Moon. *Geochim Cosmochim Acta* 139:447–471. <https://doi.org/10.1016/j.gca.2014.04.046>
- Clesi V, Ali Bouhifd M, Bolfan-Casanova N, Manthilake G, Schiavi F, Raepsaet C, Bureau H, Khodja H, Andraut D (2018) Low hydrogen contents in the cores of terrestrial planets. *Sci Adv* 4(3):e1701876. <https://doi.org/10.1126/sciadv.1701876>
- Clinton JF, Ceylan S, van Driel M, Giardini D, Stähler SC, Böse M, Charalambous C, Dahmen NL, Horleston A, Kawamura T, Khan A, Orhand-Mainsant G, Scholz JR, Euchner F, Banerdt WB, Lognonné P, Banfield D, Beucler E, Garcia RF, Kedar S, Panning MP, Perrin C, Pike WT, Smrekar SE, Spiga A, Stott AE (2021) The marsquake catalogue from InSight. *Phys Earth Planet Inter* 310:106595. <https://doi.org/10.1016/j.pepi.2020.106595>
- Connerney JEP, Acuña MH, Wasilewski PJ, Ness NF, Mazelle C, Vignes D, Lin RP, Mitchell D, Cloutier P (1999) Magnetic lineations in the ancient crust of Mars. *Science* 284(5415):794–798. <https://doi.org/10.1126/science.284.5415.794>
- Cottaar S, Koelemeijer P (2021) The interior of Mars revealed. *Science* 373(6553):388–389. <https://doi.org/10.1126/science.abj8914>
- Dauphas N, Pourmand A (2015) Thulium anomalies and rare earth element patterns in meteorites and Earth: nebular fractionation and the nugget effect. *Geochim Cosmochim Acta* 163:234–261. <https://doi.org/10.1016/j.gca.2015.03.037>
- Elkins-Tanton LT, Parmentier EM, Hess PC (2003) Magma ocean fractional crystallization and cumulate overturn in terrestrial planets: implications for Mars. *Meteorit Planet Sci* 38(12):1753–1771. <https://doi.org/10.1111/j.1945-5100.2003.tb00013.x>
- Fei Y, Bertka C (2005) The interior of Mars. *Science* 308:1120–1121. <https://doi.org/10.1126/science.1110531>
- Fei YW, Brosh E (2014) Experimental study and thermodynamic calculations of phase relations in the Fe-C system at high pressure. *Earth Planet Sci Lett* 408:155–162. <https://doi.org/10.1016/j.epsl.2014.09.044>

Acuña MH, Connerney JEP, Ness NF, Lin RP, Mitchell D, Carlson CW, McFadden J, Anderson KA, Rème H, Mazelle C, Vignes D, Wasilewski P, Cloutier P (1999) Global distribution of crustal

- Fei YW, Li J, Bertka CM, Prewitt CT (2000) Structure type and bulk modulus of Fe<sub>3</sub>S, a new iron-sulfur compound. *Am Mineral* 85(11–12):1830–1833. <https://doi.org/10.2138/am-2000-11-1229>
- Fei Y, Zhang L, Komabayashi T et al (2006) Evidences for a liquid Martian core. In 37th Lunar Planet Sci Conf Abstract#1500.
- Fischer RA, Nakajima Y, Campbell AJ, Frost DJ, Harries D, Langenhorst F, Miyajima N, Pollok K, Rubie DC (2015) High pressure metal–silicate partitioning of Ni, Co, V, Cr, Si, and O. *Geochim Cosmochim Acta* 167:177–194. <https://doi.org/10.1016/j.gca.2015.06.026>
- Gellert R, Rieder R, Brückner J, Clark BC, Dreibus G, Klingelhöfer G, Lugmair G, Ming DW, Wänke H, Yen A, Zipfel J, Squyres SW (2006) Alpha particle X-ray spectrometer (APXS): results from Gusev crater and calibration report. *J Geophys Res* 111(E2):2005JE002555. <https://doi.org/10.1029/2005je002555>
- Gendre H, Badro J, Wehr N, Borensztajn S (2022) Martian core composition from experimental high-pressure metal-silicate phase equilibria. *Geochem Perspect Lett* 21:42–46. <https://doi.org/10.7185/geochemlet.2216>
- Gilfof F, Li J (2020) Thermal state and solidification regime of the Martian core: insights from the melting behavior of FeNi-S at 20 GPa. *Earth Planet Sci Lett* 541:116285. <https://doi.org/10.1016/j.epsl.2020.116285>
- Grady MM, Verchovsky AB, Wright IP (2004) Magmatic carbon in Martian meteorites: attempts to constrain the carbon cycle on Mars. *Int J Astrobiol* 3(2):117–124. <https://doi.org/10.1017/s1473550404002071>
- Greenwood JP, Blake RE (2006) Evidence for an acidic ocean on Mars from phosphorus geochemistry of Martian soils and rocks. *Geology* 34(11):953. <https://doi.org/10.1130/g22415a.1>
- Gu TT, Stagno V, Fei YW (2019) Partition coefficient of phosphorus between liquid metal and silicate melt with implications for the Martian magma ocean. *Phys Earth Planet Inter* 295:106298. <https://doi.org/10.1016/j.pepi.2019.106298>
- Heard AW, Kite ES (2020) A probabilistic case for a large missing carbon sink on Mars after 3.5 billion years ago. *Earth Planet Sci Lett* 531:116001. <https://doi.org/10.1016/j.epsl.2019.116001>
- Helffrich G (2017) Mars core structure: concise review and anticipated insights from InSight. *Prog Earth Planet Sci* 4(1):24. <https://doi.org/10.1186/s40645-017-0139-4>
- Hemingway DJ, Driscoll PE (2021) History and future of the Martian dynamo and implications of a hypothetical solid inner core. *J Geophys Res Planets* 126(4):e2020JE006663. <https://doi.org/10.1029/2020JE006663>
- Hirose K, Tagawa S, Kuwayama Y, Sinmyo R, Morard G, Ohishi Y, Genda H (2019) Hydrogen limits carbon in liquid iron. *Geophys Res Lett* 46(10):5190–5197. <https://doi.org/10.1029/2019gl082591>
- Hirose K, Wood B, Vočadlo L (2021) Light elements in the Earth's core. *Nat Rev Earth Environ* 2(9):645–658. <https://doi.org/10.1038/s43017-021-00203-6>
- Hsieh WP, Deschamps F, Tsao YC, Yoshino T, Lin JF (2024) A thermally conductive Martian core and implications for its dynamo cessation. *Sci Adv* 10(12):eadk1087. <https://doi.org/10.1126/sciadv.adk1087>
- Huang D, Li Y, Khan A, Sossi P, Giardini D, Murakami M (2023) Thermoelastic properties of liquid Fe-rich alloys under Martian core conditions. *Geophys Res Lett* 50(6):e2022GL102271. <https://doi.org/10.1029/2022GL102271>
- Irving JCE, Lekić V, Durán C, Drilleau M, Kim D, Rivoldini A, Khan A, Samuel H, Antonangeli D, Banerdt WB, Beghein C, Bozdağ E, Ceylan S, Charalambous C, Clinton J, Davis P, Garcia R, Giardini D, Horleston AC, Huang QC, Hurst KJ, Kawamura T, King SD, Knappmeyer M, Li JQ, Lognonné P, Maguire R, Panning MP, Plesa AC, Schimmel M, Schmerr NC, Stähler SC, Stutzmann E, Xu ZB (2023) First observations of core-transiting seismic phases on Mars. *Proc Natl Acad Sci U S A* 120(18):e2217090120. <https://doi.org/10.1073/pnas.2217090120>
- Jones EG (2018) Shallow transient liquid water environments on present-day Mars, and their implications for life. *Acta Astronaut* 146:144–150. <https://doi.org/10.1016/j.actaastro.2018.02.027>
- Khan A, Huang D, Durán C, Sossi PA, Giardini D, Murakami M (2023) Evidence for a liquid silicate layer atop the Martian core. *Nature* 622(7984):718–723. <https://doi.org/10.1038/s41586-023-06586-4>
- Khan A, Liebske C, Rozel A, Rivoldini A, Nimmo F, Connolly JAD, Plesa AC, Giardini D (2018) A geophysical perspective on the bulk composition of Mars. *JGR Planets* 123(2):575–611. <https://doi.org/10.1002/2017je005371>
- Khan A, Sossi PA, Liebske C, Rivoldini A, Giardini D (2022) Geophysical and cosmochemical evidence for a volatile-rich Mars. *Earth Planet Sci Lett* 578:117330. <https://doi.org/10.1016/j.epsl.2021.117330>
- Kinoshita D, Nakajima Y, Kuwayama Y, Hirose K, Iwamoto A, Ishikawa D, Baron AQR (2020) Sound velocity of liquid Fe–P at high pressure. *Phys Status Solidi B* 257(11):2000171. <https://doi.org/10.1002/pssb.202000171>
- Kite ES (2019) Geologic constraints on early Mars climate. *Space Sci Rev* 215(1):10. <https://doi.org/10.1007/s11214-018-0575-5>
- Komabayashi T (2021) Phase relations of Earth's core-forming materials. *Crystals* 11(6):581. <https://doi.org/10.3390/cryst11060581>
- Kuwayama Y, Morard G, Nakajima Y, Hirose K, Baron AQR, Kawaguchi SI, Tsuchiya T, Ishikawa D, Hirao N, Ohishi Y (2020) Equation of state of liquid iron under extreme conditions. *Phys Rev Lett* 124(16):165701. <https://doi.org/10.1103/physrevlett.124.165701>
- Lai XJ, Zhu F, Gao J, Greenberg E, Prakapenka VB, Meng Y, Chen B (2022) Melting of the Fe–C–H system and Earth's deep carbon-hydrogen cycle. *Geophys Res Lett* 49(13):e2022GL098919. <https://doi.org/10.1029/2022gl098919>
- Le Maistre S, Rivoldini A, Caldiero A, Yseboodt M, Baland RM, Beuthe M, Van Hoolst T, Dehant V, Folkner WM, Buccino D, Kahan D, Marty JC, Antonangeli D, Badro J, Drilleau M, Konopliv A, Péters MJ, Plesa AC, Samuel H, Tosi N, Wieczorek M, Lognonné P, Panning M, Smrekar S, Banerdt WB (2023) Spin state and deep interior structure of Mars from InSight radio tracking. *Nature* 619(7971):733–737. <https://doi.org/10.1038/s41586-023-06150-0>
- Li J, Fei Y (2014) Experimental constraints on core composition. *Treatise on Geochemistry*. Elsevier, Amsterdam, pp 527–557
- Li WJ, Li Z, Ma Z, Zhou J, Wang C, Zhang P (2024a) Thermoelastic properties and thermal evolution of the Martian core from *ab initio* calculated magnetic Fe–S liquid. *J Geophys Res Planets* 129(4):e2023JE007874. <https://doi.org/10.1029/2023JE007874>
- Li XH, Han SS, Cui XM, Liu J, Hou MQ (2024b) Sound velocities of Fe–Si alloys at conditions of the cores of moon and mercury. *J Geophys Res Planets* 129(4):e2023JE008005. <https://doi.org/10.1029/2023JE008005>
- Li Y, Dasgupta R, Tsuno K (2015) The effects of sulfur, silicon, water, and oxygen fugacity on carbon solubility and partitioning in Fe-rich alloy and silicate melt systems at 3 GPa and 1600 °C: implications for core–mantle differentiation and degassing of magma oceans and reduced planetary mantles. *Earth Planet Sci Lett* 415:54–66. <https://doi.org/10.1016/j.epsl.2015.01.017>
- Li Y, Dasgupta R, Tsuno K, Monteleone B, Shimizu N (2016) Carbon and sulfur budget of the silicate Earth explained by accretion of differentiated planetary embryos. *Nat Geosci* 9(10):781–785. <https://doi.org/10.1038/ngeo2801>
- Li YG, Li CH, Zhou Y, Liu Y, Ni HW (2025) A deeper and hotter Martian core–mantle differentiation inferred from FeO partitioning.

- Sci Bull 70(3):429–436. <https://doi.org/10.1016/j.scib.2024.11.046>
- Liu J, Lin JF, Prakapenka VB, Prescher C, Yoshino T (2016) Phase relations of Fe<sub>3</sub>C and Fe<sub>7</sub>C<sub>3</sub> up to 185 GPa and 5200 K: implication for the stability of iron carbide in the Earth's core. *Geophys Res Lett* 43(24):12415–12422. <https://doi.org/10.1002/2016GL071353>
- Liu T, Jing ZC (2025) Limited influence of hydrogen on the sound velocity of the Martian core: constraints from first-principles molecular dynamics simulations of Fe-S-H liquids. *J Geophys Res Planets* 130(1):e2024JE008552. <https://doi.org/10.1029/2024JE008552>
- Man LJ, Li X, Boffa Ballaran T, Zhou WJ, Chantel J, Néri A, Kupenko I, Aprilis G, Kurnosov A, Namur O, Hanfland M, Guignot N, Henry L, Dubrovinsky L, Frost DJ (2025) The structure and stability of Fe<sub>4+x</sub>S<sub>3</sub> and its potential to form a Martian inner core. *Nat Commun* 16:1710. <https://doi.org/10.1038/s41467-025-56220-2>
- Martín-Torres FJ, Zorzano MP, Valentín-Serrano P, Harri AM, Genzer M, Kempainen O, Rivera-Valentín EG, Jun I, Wray J, Bo Madsen M, Goetz W, McEwen AS, Hardgrove C, Renno N, Chevrier VF, Mischna M, Navarro-González R, Martínez-Frías J, Conrad P, McConnochie T, Cockell C, Berger G, Vasavada R, A, Sumner D, Vaniman D, (2015) Transient liquid water and water activity at Gale crater on Mars. *Nat Geosci* 8(5):357–361. <https://doi.org/10.1038/ngeo2412>
- Ming DW, Gellert R, Morris RV, Arvidson RE, Brückner J, Clark BC, Cohen BA, d'Uston C, Economou T, Fleischer I, Klingelhöfer G, McCoy TJ, Mittlefehldt DW, Schmidt ME, Schröder C, Squyres SW, Tréguier E, Yen AS, Zipfel J (2008) Geochemical properties of rocks and soils in Gusev crater, Mars: results of the alpha particle X-ray spectrometer from Cumberland ridge to home plate. *J Geophys Res* 113(E12):2008JE003195. <https://doi.org/10.1029/2008je003195>
- Mittelholz A, Johnson CL, Feinberg JM, Langlais B, Phillips RJ (2020) Timing of the Martian dynamo: new constraints for a core field 4.5 and 3.7 Ga ago. *Sci Adv* 6(18):eaba0513. <https://doi.org/10.1126/sciadv.aba0513>
- Morard G, Andrault D, Antonangeli D, Nakajima Y, Auzende AL, Boulard E, Cervera S, Clark A, Lord OT, Siebert J, Svitlyk V, Garbarino G, Mezouar M (2017) Fe–FeO and Fe–Fe<sub>3</sub>C melting relations at Earth's core–mantle boundary conditions: implications for a volatile-rich or oxygen-rich core. *Earth Planet Sci Lett* 473:94–103. <https://doi.org/10.1016/j.epsl.2017.05.024>
- Nakajima Y, Imada S, Hirose K, Komabayashi T, Ozawa H, Tateno S, Tsutsui S, Kuwayama Y, Baron AQR (2015) Carbon-depleted outer core revealed by sound velocity measurements of liquid iron-carbon alloy. *Nat Commun* 6:8942. <https://doi.org/10.1038/ncomms9942>
- Nazari-Sharabian M, Aghababaei M, Karakouzian M, Karami M (2020) Water on Mars: a literature review. *Galaxies* 8(2):40. <https://doi.org/10.3390/galaxies8020040>
- Newsom HE, Drake MJ (1983) Experimental investigation of the partitioning of phosphorus between metal and silicate phases: implications for the Earth, Moon and Eucrite Parent Body. *Geochim Cosmochim Acta* 47(1):93–100. [https://doi.org/10.1016/0016-7037\(83\)90093-5](https://doi.org/10.1016/0016-7037(83)90093-5)
- Nishida K, Shibazaki Y, Terasaki H, Higo Y, Suzuki A, Funamori N, Hirose K (2020) Effect of sulfur on sound velocity of liquid iron under Martian core conditions. *Nat Commun* 11(1):1954. <https://doi.org/10.1038/s41467-020-15755-2>
- Nishida K, Suzuki A, Terasaki H, Shibazaki Y, Higo Y, Kuwabara S, Shimoyama Y, Sakurai M, Ushioda M, Takahashi E, Kikegawa T, Wakabayashi D, Funamori N (2016) Towards a consensus on the pressure and composition dependence of sound velocity in the liquid Fe–S system. *Phys Earth Planet Inter* 257:230–239. <https://doi.org/10.1016/j.pepi.2016.06.009>
- Ohta K, Kuwayama Y, Hirose K, Shimizu K, Ohishi Y (2016) Experimental determination of the electrical resistivity of iron at Earth's core conditions. *Nature* 534(7605):95–98. <https://doi.org/10.1038/nature17957>
- Ohtani E, Ringwood AE, Hibberson W (1984) Composition of the core, part II. effect of high pressure on solubility of FeO in molten iron. *Earth Planet Sci Lett* 71(1):94–103. [https://doi.org/10.1016/0012-821X\(84\)90055-4](https://doi.org/10.1016/0012-821X(84)90055-4)
- Oka K, Ikuta N, Tagawa S, Hirose K, Ohishi Y (2022) Melting experiments on Fe–O–H and Fe–H: evidence for eutectic melting in Fe–FeH and implications for hydrogen in the core. *Geophys Res Lett* 49(17):e2022GL099420. <https://doi.org/10.1029/2022GL099420>
- Piet H, Leinenweber K, Greenberg E, Prakapenka VB, Shim SH (2021) Effects of hydrogen on the phase relations in Fe–FeS at pressures of Mars-sized bodies. *J Geophys Res Planets* 126(11):e2021JE006942. <https://doi.org/10.1029/2021JE006942>
- Pommier A, Laurenz V, Davies CJ, Frost DJ (2018) Melting phase relations in the Fe–S and Fe–S–O systems at core conditions in small terrestrial bodies. *Icarus* 306:150–162. <https://doi.org/10.1016/j.icarus.2018.01.021>
- Rai N, van Westrenen W (2013) Core–mantle differentiation in Mars. *J Geophys Res Planets* 118(6):1195–1203. <https://doi.org/10.1002/jgre.20093>
- Ricolleau A, Fei YW, Corgne A, Siebert J, Badro J (2011) Oxygen and silicon contents of Earth's core from high pressure metal–silicate partitioning experiments. *Earth Planet Sci Lett* 310(3–4):409–421. <https://doi.org/10.1016/j.epsl.2011.08.004>
- Righter K, Chabot NL (2011) Moderately and slightly siderophile element constraints on the depth and extent of melting in early Mars. *Meteorit Planet Sci* 46(2):157–176. <https://doi.org/10.1111/j.1945-5100.2010.01140.x>
- Rivoldini A, Van Hoolst T, Verhoeven O, Mocquet A, Dehant V (2011) Geodesy constraints on the interior structure and composition of Mars. *Icarus* 213(2):451–472. <https://doi.org/10.1016/j.icarus.2011.03.024>
- Sakamaki K, Takahashi E, Nakajima Y, Nishihara Y, Funakoshi K, Suzuki T, Fukai Y (2009) Melting phase relation of FeH<sub>x</sub> up to 20 GPa: implication for the temperature of the Earth's core. *Phys Earth Planet Inter* 174(1–4):192–201. <https://doi.org/10.1016/j.pepi.2008.05.017>
- Sakamaki T, Ohtani E, Fukui H, Kamada S, Takahashi S, Sakairi T, Takahata A, Sakai T, Tsutsui S, Ishikawa D, Shiraishi R, Seto Y, Tsuchiya T, Baron AQR (2016) Constraints on Earth's inner core composition inferred from measurements of the sound velocity of hcp-iron in extreme conditions. *Sci Adv* 2(2):e1500802. <https://doi.org/10.1126/sciadv.1500802>
- Samuel H, Ballmer MD, Padovan S, Tosi N, Rivoldini A, Plesa AC (2021) The thermo-chemical evolution of Mars with a strongly stratified mantle. *J Geophys Res Planets* 126(4):e2020JE006613. <https://doi.org/10.1029/2020JE006613>
- Samuel H, Drilleau M, Rivoldini A, Xu ZB, Huang QC, Garcia RF, Lekić V, Irving JCE, Badro J, Lognonné PH, Connolly JAD, Kawamura T, Gudkova T, Banerdt WB (2023) Geophysical evidence for an enriched molten silicate layer above Mars's core. *Nature* 622(7984):712–717. <https://doi.org/10.1038/s41586-023-06601-8>
- Shen GY, Lazor P, Saxena SK (1993) Melting of wüstite and iron up to pressures of 600 kbar. *Phys Chem Miner* 20(2):91–96. <https://doi.org/10.1007/BF00207201>
- Shen GY, Mao HK, Hemley RJ, Duffy TS, Rivers ML (1998) Melting and crystal structure of iron at high pressures and temperatures. *Geophys Res Lett* 25(3):373–376. <https://doi.org/10.1029/97GL03776>

- Shibazaki Y, Ohtani E, Terasaki H, Suzuki A, Funakoshi KI (2009) Hydrogen partitioning between iron and ringwoodite: implications for water transport into the Martian core. *Earth Planet Sci Lett* 287(3–4):463–470. <https://doi.org/10.1016/j.epsl.2009.08.034>
- Siebert J, Corgne A, Ryerson FJ (2011) Systematics of metal-silicate partitioning for many siderophile elements applied to Earth's core formation. *Geochim Cosmochim Acta* 75:1451–1489. <https://doi.org/10.1016/j.gca.2010.12.013>
- Siebert J, Badro J, Antonangeli D, Ryerson FJ (2013) Terrestrial accretion under oxidizing conditions. *Science* 339(6124):1194–1197. <https://doi.org/10.1126/science.1227923>
- Skála R, Císařová I (2005) Crystal structure of meteoritic schreibersites: determination of absolute structure. *Phys Chem Miner* 31(10):721–732. <https://doi.org/10.1007/s00269-004-0435-6>
- Smrekar SE, Lognonné P, Spohn T, Banerdt WB, Breuer D, Christensen U, Dehant V, Drilleau M, Folkner W, Fuji N, Garcia RF, Giardini D, Golombek M, Grott M, Gudkova T, Johnson C, Khan A, Langlais B, Mittelholz A, Mocquet A, Myhill R, Panning M, Perrin C, Pike T, Plesa AC, Rivoldini A, Samuel H, Stähler SC, van Driel M, Van Hoolst T, Verhoeven O, Weber R, Wiczeorek M (2019) Pre-mission insights on the interior of Mars. *Space Sci Rev* 215:3. <https://doi.org/10.1007/s11214-018-0563-9>
- Sohl F, Spohn T (1997) The interior structure of Mars: implications from SNC meteorites. *J Geophys Res Planets* 102(E1):1613–1635. <https://doi.org/10.1029/96JE03419>
- Stähler SC, Khan A, Banerdt WB, Lognonné P, Giardini D, Ceylan S, Drilleau M, Duran AC, Garcia RF, Huang QC, Kim D, Lekic V, Samuel H, Schimmel M, Schmerr N, Sollberger D, Stutzmann É, Xu ZB, Antonangeli D, Charalambous C, Davis PM, Irving JCE, Kawamura T, Knapmeyer M, Maguire R, Marusiak AG, Panning MP, Perrin C, Plesa AC, Rivoldini A, Schmelzbach C, Zenhäuser G, Beucler É, Clinton J, Dahmen N, van Driel M, Gudkova T, Horleston A, Pike WT, Plasman M, Smrekar SE (2021) Seismic detection of the Martian core. *Science* 373(6553):443–448. <https://doi.org/10.1126/science.abi7730>
- Steenstra ES, van Westrenen W (2018) A synthesis of geochemical constraints on the inventory of light elements in the core of Mars. *Icarus* 315:69–78. <https://doi.org/10.1016/j.icarus.2018.06.023>
- Stevenson DJ (2001) Mars' core and magnetism. *Nature* 412(6843):214–219. <https://doi.org/10.1038/35084155>
- Stewart AJ, Schmidt MW (2007) Sulfur and phosphorus in the Earth's core: the Fe–P–S system at 23 GPa. *Geophys Res Lett* 34(13):2007GL030138. <https://doi.org/10.1029/2007GL030138>
- Stewart AJ, Schmidt MW, van Westrenen W, Liebske C (2007) Mars: a new core-crystallization regime. *Science* 316(5829):1323–1325. <https://doi.org/10.1126/science.1140549>
- Suzuki T, Akimoto SI, Fukai Y (1984) The system iron-enstatite-water at high pressures and temperatures: formation of iron hydride and some geophysical implications. *Phys Earth Planet Inter* 36(2):135–144. [https://doi.org/10.1016/0031-9201\(84\)90014-1](https://doi.org/10.1016/0031-9201(84)90014-1)
- Takahashi S, Ohtani E, Terasaki H, Ito Y, Shibazaki Y, Ishii M, Funakoshi KI, Higo Y (2013) Phase relations in the carbon-saturated C–Mg–Fe–Si–O system and C and Si solubility in liquid Fe at high pressure and temperature: implications for planetary interiors. *Phys Chem Miner* 40(8):647–657. <https://doi.org/10.1007/s00269-013-0600-x>
- Terasaki H, Rivoldini A, Shimoyama Y, Nishida K, Urakawa S, Maki M, Kurokawa F, Takubo Y, Shibazaki Y, Sakamaki T, Machida A, Higo Y, Uesugi K, Takeuchi A, Watanuki T, Kondo T (2019) Pressure and composition effects on sound velocity and density of core-forming liquids: implication to core compositions of terrestrial planets. *JGR Planets* 124(8):2272–2293. <https://doi.org/10.1029/2019je005936>
- Tsuno K, Frost DJ, Rubie DC (2011) The effects of nickel and sulphur on the core–mantle partitioning of oxygen in Earth and Mars. *Phys Earth Planet Inter* 185(1–2):1–12. <https://doi.org/10.1016/j.pepi.2010.11.009>
- Tsuno K, Grewal DS, Dasgupta R (2018) Core-mantle fractionation of carbon in Earth and Mars: the effects of sulfur. *Geochim Cosmochim Acta* 238:477–495. <https://doi.org/10.1016/j.gca.2018.07.010>
- Umamoto K, Hirose K (2020) Chemical compositions of the outer core examined by first principles calculations. *Earth Planet Sci Lett* 531:116009. <https://doi.org/10.1016/j.epsl.2019.116009>
- Wei XH, Chariton S, Prakapenka VB, Fei YW, Shim D (2024) Effects of hydrogen on Fe–S alloys and their implications for the Martian core. *ESS Open Archive* <https://doi.org/10.22541/essoar.172163245.54357819/v1>
- Wood BJ, Li J, Shahar A (2013) Carbon in the core: its influence on the properties of core and mantle. *Rev Mineral Geochem* 75(1):231–250. <https://doi.org/10.2138/rmg.2013.75.8>
- Yamada I, Terasaki H, Urakawa S, Kondo T, Machida A, Tange Y, Higo Y (2023) Sound velocity and elastic properties of Fe–Ni–S–Si liquid: the effects of pressure and multiple light elements. *Phys Chem Miner* 50(3):19. <https://doi.org/10.1007/s00269-023-01243-8>
- Yokoo S, Hirose K (2024) Melting experiments on Fe–S–O–C alloys at Martian core conditions: possible structures in the O- and C-bearing core of Mars. *Geochim Cosmochim Acta* 378:234–244. <https://doi.org/10.1016/j.gca.2024.06.027>
- Yoshizaki T, McDonough WF (2020) The composition of Mars. *Geochim Cosmochim Acta* 273:137–162. <https://doi.org/10.1016/j.gca.2020.01.011>
- Yuan L, Steinle-Neumann G (2023) Hydrogen distribution between the Earth's inner and outer core. *Earth Planet Sci Lett* 609:118084. <https://doi.org/10.1016/j.epsl.2023.118084>
- Zambardi T, Poitrasson F, Corgne A, Méheut M, Quitté G, Anand M (2013) Silicon isotope variations in the inner solar system: implications for planetary formation, differentiation and composition. *Geochim Cosmochim Acta* 121:67–83. <https://doi.org/10.1016/j.gca.2013.06.040>
- Zhang DZ, Jackson JM, Zhao JY, Sturhahn W, Alp EE, Hu MY, Toellner TS, Murphy CA, Prakapenka VB (2016) Temperature of Earth's core constrained from melting of Fe and Fe<sub>0.9</sub>Ni<sub>0.1</sub> at high pressures. *Earth Planet Sci Lett* 447:72–83. <https://doi.org/10.1016/j.epsl.2016.04.026>
- Zhang L, Fei YW (2008) Effect of Ni on Fe–FeS phase relations at high pressure and high temperature. *Earth Planet Sci Lett* 268(1–2):212–218. <https://doi.org/10.1016/j.epsl.2008.01.028>

**Publisher's Note** Springer Nature remains neutral with regard to jurisdictional claims in published maps and institutional affiliations.

Springer Nature or its licensor (e.g. a society or other partner) holds exclusive rights to this article under a publishing agreement with the author(s) or other rightsholder(s); author self-archiving of the accepted manuscript version of this article is solely governed by the terms of such publishing agreement and applicable law.